



# Effect of chemical degradation on fluxes of reactive compounds – a study with a stochastic Lagrangian transport model

J. Rinne<sup>1</sup>, T. Markkanen<sup>2</sup>, T. M. Ruuskanen<sup>1</sup>, T. Petäjä<sup>1</sup>, P. Keronen<sup>1</sup>, M.J. Tang<sup>3</sup>, J. N. Crowley<sup>3</sup>, Ü. Rannik<sup>2</sup>, and T. Vesala<sup>3</sup>

<sup>1</sup>University of Helsinki, Department of Physics, Finland

<sup>2</sup>Finnish Meteorological Institute, Helsinki, Finland

<sup>3</sup>Max-Planck-Institute for Chemistry, Division of Atmospheric Chemistry, Mainz, Germany

Correspondence to: J. Rinne. (janne.rinne@helsinki.fi)

Received: 21 November 2011 – Published in Atmos. Chem. Phys. Discuss.: 2 December 2011

Revised: 3 May 2012 – Accepted: 7 May 2012 – Published: 1 June 2012

**Abstract.** In the analyses of VOC fluxes measured above plant canopies, one usually assumes the flux above canopy to equal the exchange at the surface. Thus one assumes the chemical degradation to be much slower than the turbulent transport. We used a stochastic Lagrangian transport model in which the chemical degradation was described as first order decay in order to study the effect of the chemical degradation on above canopy fluxes of chemically reactive species. With the model we explored the sensitivity of the ratio of the above canopy flux to the surface emission on several parameters such as chemical lifetime of the compound, friction velocity, stability, and canopy density. Our results show that friction velocity and chemical lifetime affected the loss during transport the most. The canopy density had a significant effect if the chemically reactive compound was emitted from the forest floor. We used the results of the simulations together with oxidant data measured during HUMPPA-COPEC-2010 campaign at a Scots pine site to estimate the effect of the chemistry on fluxes of three typical biogenic VOCs, isoprene,  $\alpha$ -pinene, and  $\beta$ -caryophyllene. Of these, the chemical degradation had a major effect on the fluxes of the most reactive species  $\beta$ -caryophyllene, while the fluxes of  $\alpha$ -pinene were affected during nighttime. For these two compounds representing the mono- and sesquiterpenes groups, the effect of chemical degradation had also a significant diurnal cycle with the highest chemical loss at night. The different day and night time loss terms need to be accounted for, when measured fluxes of reactive compounds are used to reveal relations between primary emission and environmental parameters.

## 1 Introduction

While micrometeorological flux measurement techniques are commonly used to measure exchange of e.g. carbon dioxide, water vapour and methane between ecosystems and atmosphere, they are also applied to an increasing degree to the emissions of chemically reactive species, such as volatile organic compounds (VOC), from different ecosystems (Fowler et al., 2009; Kesselmeier et al., 2009; Rinne et al., 2009). These above canopy fluxes are also used to infer functional dependencies of VOC emissions on environmental parameters such as temperature and solar radiation (e.g. Rinne et al., 2002; Hörtnagl et al., 2011; Taipale et al., 2011). When interpreting the measured fluxes of e.g. VOCs, the chemical lifetime of a compound is commonly assumed to be much longer than the transport time leading to correspondence of measured flux and surface exchange. However, there are compounds emitted by e.g. vegetation with lifetimes comparable to the transport time, such as  $\beta$ -caryophyllene, a sesquiterpene. The chemical degradation of these compounds below the flux measurement level can lead to a significantly lower measured flux as compared to the actual emission from the vegetation surfaces (Ciccioli et al., 1999).

Commonly, the Damköhler number (Damköhler, 1940) has been used to assess the potential importance of atmospheric chemistry on fluxes. The Damköhler number is the ratio of the time scale of turbulent mixing to the chemical lifetime of a compound. Thus, the larger the Damköhler number is, the more likely is it for the chemical degradation to cause significant reduction to above canopy fluxes. However,

this approach can only be used to classify the situation in a semi-quantitative way as it does not yield quantitative value for the flux loss due to the chemical degradation. Furthermore, it is not clear whether the simple estimates of mixing time-scale applies to deep and dense canopies, as friction velocity that is determined for a height above canopy may not be a proper scaling parameter for within and below-canopy turbulence (e.g. Launiainen et al., 2005). Models with detailed descriptions of turbulent transport and chemistry in the atmospheric surface layer, which could be used to assess the problem already exist (Boy et al., 2011). However, these models often utilize K-theory (see e.g. Stull, 1988) for mixing the chemical species and thus they may not describe the mixing within and below canopy in an appropriate way.

Stochastic Lagrangian models of turbulent transport in the atmospheric surface layer have been previously applied for estimation of flux footprint functions (e.g. Vesala et al., 2008; Rannik et al., 2012). In these models air parcels are released from a certain level within the vegetation and their path is followed as they are transported by both the mean horizontal wind and the turbulent fluctuations. The distribution of horizontal distances from the release to transport across measurement level yields the footprint function. The mean wind and turbulence profiles are typically constrained and are based either on observations or on numerical simulations.

More recently the stochastic Lagrangian transport models have been applied to study the effect of the chemical degradation on above canopy fluxes of volatile organic compounds emitted by vegetation (Strong et al., 2004; Rinne et al., 2007). In this approach the initial concentration of a reactive compound in each air parcel was reduced by first order decay. When the air parcel is transported across the measurement level its remaining concentration is recorded. The flux-to-emission ( $F/E$ ) ratio is then obtained as the ratio of the sum of recorded crossings weighted by their remaining concentrations to the sum of releases multiplied by the initial concentration.

In the study by Rinne et al. (2007) a significant flux reduction was observed already at Damköhler number around 0.1. However, in that study the results were presented for a specific canopy height, canopy density and friction velocity. Also only neutral stratification was considered. Our aim is to generalize the earlier paper by presenting the results in normalized forms, and to expand it by studying the sensitivity of the chemical flux degradation on atmospheric conditions, stability and friction velocity, and site specific parameters, canopy density, depth and structure.

## 2 Theory and modeling

In ideal conditions when all the assumptions made during the derivation of the flux equation from the scalar conservation equation are valid, the flux we are measuring ( $F$ ) equals the surface exchange ( $E$ ) we are interested in. In this case

the ratio of flux to surface exchange, i.e.  $F/E$  ratio, equals to unity. Chemical transformations are but one process deviating the  $F/E$  ratio from unity, others being e.g. advection and storage change. In the case of chemical degradation of e.g. VOCs emitted from surface, the  $F/E$  ratio becomes less than unity, whereas in the case of e.g. ozone deposition and simultaneous chemical destruction below flux measurement level the  $F/E$  ratio can be above unity. Below we describe the application of a stochastic Lagrangian transport model with chemistry described as first-order-decay to determination of  $F/E$  ratios for reactive gas emissions. The methodology applies to those atmospheric compounds whose lifetimes can be described by simple first order differential equation.

### 2.1 Chemical lifetime and turbulent mixing timescale

The change of the concentration of a compound  $X$  in Lagrangian framework and in absence of source terms can be written for a first order reaction as

$$\frac{D[X]}{Dt} = \sum_i k_{X,i} [X] [R_i] \quad (1)$$

where  $[R_i]$  is the concentration of an oxidant,  $[X]$  is the concentration of compound  $X$ , and  $k_{X,i}$  is the reaction rate constant between the oxidant and the compound in question. This can be solved to yield

$$[X] = [X]_0 \exp(-t/\tau_c) \quad (2)$$

where  $[X]_0$  is the concentration in the beginning and  $\tau_c$  is the chemical life time of the compound  $X$ , which can be written as

$$\tau_c = \left( \sum_i k_i [R_i] \right)^{-1}. \quad (3)$$

In the case of VOCs this can be written as

$$\tau_c = (k_{X,OH} [OH] + k_{X,O_3} [O_3] + k_{X,NO_3} [NO_3] + k_{X,photolysis})^{-1} \quad (4)$$

where OH is hydroxyl radical,  $O_3$  ozone, and  $NO_3$  nitrate radical. We have also included the photolysis rate of the compound,  $k_{X,photolysis}$ .

The ratio of the mixing timescale to the chemical timescale, i.e. Damköhler number, can be written as

$$Da = \frac{\tau_t}{\tau_c} \quad (5)$$

where  $\tau_t$  is the mixing timescale (Damköhler, 1940). In the case of a Damköhler number well below unity, the chemical timescale is much longer than the mixing timescale and the flux at the measurement height corresponds to the emission. If the Damköhler number is above unity the chemical timescale is shorter than the mixing timescale and the flux at measurement height will be lower than the primary emission.

The mixing time-scale can be roughly estimated as

$$\tau_t = \frac{z}{u_*} \quad (6)$$

where  $z$  is the measurement height and  $u_*$  is the friction velocity (e.g. Rinne et al., 2000). While the Damköhler number as described by Eqs. (5) and (6) is useful as a practical metric it may not be suitable for dense canopies, as above canopy friction velocity is not a proper scaling parameter for below canopy turbulence and as the chemical lifetime in such environments can have strong vertical gradients.

## 2.2 Stochastic Lagrangian Transport Chemistry model

Stochastic Lagrangian transport models describe the movement of air parcels in the surface layer. In these, the movement is divided to two parts. First, the deterministic part depends on the mean wind profile and is typically purely horizontal. The second part of the movement represents the turbulent motion and is described as random step, which can have both horizontal and vertical components. The statistics of these random movements depend on the profile of turbulence statistics. Wind and turbulence statistic profiles are pre-described and can be taken from a canopy – surface layer model (e.g. Massman and Weill, 1999) or from measurements. While Massman and Weill (1999) model reproduces the above canopy profiles reasonably well, it predicts standard deviation of vertical velocity inside the canopy to be constant, which is not supported by measurements inside forest canopies (Rannik et al., 2003). Also the basal layer may not be well represented in the model. However, only few datasets consisting of turbulence statistics at sufficient vertical resolution both inside and above forest canopies exist, and one typically uses modeled wind and turbulence profiles.

In this study, in order to predict fluxes of gaseous tracers, a large number (50 000) of Lagrangian stochastic air parcels (or particles) were dispersed forward in time according to Thomson's (1987) 3-D diffusion model. The vertical profiles of the first and the second order variables characterizing the stationary flow-fields inside the vegetation canopy were determined with the 1D model of Massman and Weil (1999). The atmospheric stability was accounted for by universal stability functions of second order flow statistics, wind speed and dissipation rate within the atmospheric surface layer (ASL). The used stochastic Lagrangian transport chemistry (SLTC) model described the chemical degradation as first order decay. A detailed description of the stability functions together with their parameter values are given in Rannik et al. (2001). The vertical leaf area distribution (LAD) used to constrain the Massman (1997) model was defined by a normalized beta-distribution in a manner presented in Markkanen et al. (2003).

$$\text{LAD}(z_n) = \frac{z_n^{\alpha-1} (1 - z_n)^{\beta-1}}{\int_0^1 z_n^{\alpha-1} (1 - z_n)^{\beta-1} dz_n} \quad (7)$$

**Table 1.** Canopy parameters for pine and spruce.

	Pine	Spruce
Parameter $\alpha$ of beta distribution of leaf area distribution (LAD)	10	2
Displacement height ( $d/h$ )	0.78	0.5
Roughness length ( $z/h$ )	0.97	0.16

where  $z_n$  is the height normalized with canopy height ( $z_n = z/h$ ). In this study the parameter  $\beta$  was set to a constant value of 3 while  $\alpha$  was varied in order to describe various canopy shapes. The lower the  $\alpha$  is, the closer to forest floor is the peak of the LAD located at (Markkanen et al., 2003). In the most of simulations presented this study the LAI and  $\alpha$  were set equal to those used in Rannik et al. (2003) having values  $3.5 \text{ m}^2 \text{ m}^{-2}$  and 10, respectively. The resulting canopy shape and density thus closely resemble those of a middle-aged Scots pine canopy in Southern Finland. The LAI was varied from  $1.75 \text{ m}^2 \text{ m}^{-2}$  to  $7.0 \text{ m}^2 \text{ m}^{-2}$  for simulations used to study the effect of canopy density on  $F/E$  ratios. In order to simulate spruce forest canopy the LAI was set to  $3.5 \text{ m}^2 \text{ m}^{-2}$  and  $\alpha$  to 2. The normalised displacement heights and roughness lengths predicted by the model of Massman (1997) in both LAD cases are given in Table 1. Like all the variables with dimension of length, these are also normalised by canopy height.

In both cases two tracer source heights were considered; forest floor, i.e. 0.005 times the canopy height ( $h$ ) and 0.8 times canopy height ( $h$ ). This is close to displacement height of  $0.78 \times h$  predicted by the Massman (1997) model in the “Scots pine” case. Simulated particles are perfectly reflected at the forest floor.

In the case of inert tracer a dispersing particle contributes to the flux at a horizontal level each time it crosses the level. The flux  $F$  at a horizontal level of interest ( $z_m$ ) at a location ( $x, y$ ) is given by

$$F(x, y, z_m) = \frac{1}{N} \sum_{i=1}^N \sum_{j=1}^{n_i} \frac{w_{ij}}{|w_{ij}|} E(x - X_{ij}, y - Y_{ij}, z_s) \quad (8)$$

where  $N$  is the number of particles released in the model,  $n_i$  stands for number of interceptions of the particle with the observation level  $z_m$   $w_{ij}$ ,  $X_{ij}$  and  $Y_{ij}$  denote the vertical velocity and the coordinates of particle  $i$  at the intersection moment, respectively and  $E$  is the emission source as a function of location, (see e.g. Vesala et al., 2008; Rannik et al., 2012). Integration of the right hand side of this equation horizontally to infinity yields the total emission. In practice, in the simulations, the parcels are followed for so long, that the surface layer flux of inert tracer at the observation level reaches 95% of the emission or more. Here it is assumed that the parcels leaving the surface layer do not return there, which does not hold for instance under a convective situation, that is governed by large coherent up and down dwelling structures.

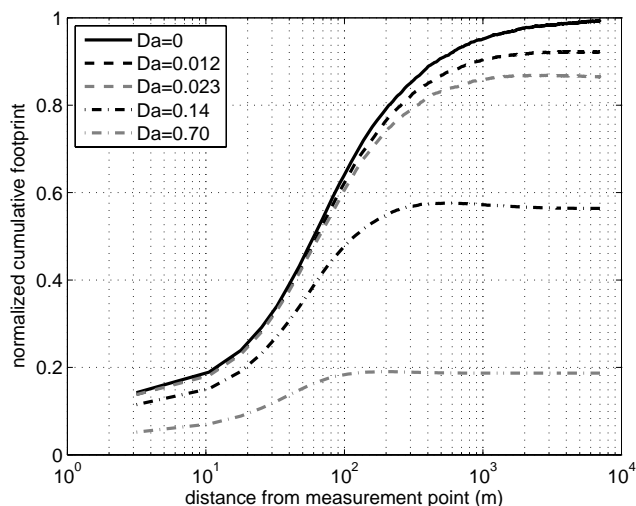


**Fig. 1.** Example of cumulative flux footprints for inert and reactive gases as calculated by the SLTC-model for height of 1.5 times the canopy height. The cumulative footprint of the inert compound ( $Da = 0$ ) approaches unity while the others are affected by the chemical degradation.

In order to estimate the effect of the chemical degradation on the fluxes we give each air parcel in the model an initial concentration value  $\phi = 1$  at the time of release. This concentration is then decreased at each time-step as

$$\phi_k = \phi_{k-1} \exp(-\Delta t / \tau_c) \quad (9)$$

where  $\phi_k$  is the concentration at the time step  $k$ ,  $\phi_{k-1}$  the concentration in the previous time step, and  $\Delta t$  is the length of the time step. We also consider the emission source to be horizontally homogenous,  $E(z_s)$ , depending only on height,  $z_s$ . The flux of a reactive compound at a height  $z_m$  is thus given by

$$F(z_m) = \frac{1}{N} \sum_{i=1}^N \sum_{j=1}^{n_i} \frac{w_{ij}}{|w_{ij}|} \phi(R_{ij}) E(z_s) \quad (10)$$

where  $R_{ij}$  denotes the path the air parcel has traveled before interception. Integration horizontally to infinity does yield values lower than unity, depending on the chemical lifetime and travel time and path of air parcels. Normalization of the Eq. (10) by dividing with source strength yields an expression to calculate the  $F/E$  ratio with our model.

A cumulative footprint function for inert compound and for compounds with different chemical lifetimes is presented in Fig. 1. From this figure one can see how the cumulative footprint of the inert compound approaches unity while those for reactive compounds do not. The asymptotic value of the cumulative footprint is thus the ratio of the flux to the primary emission.

As the parameters in the model are represented in unitless normalized form, the chemical lifetime is also presented in the model as

$$\tau_c^N = \frac{u_* \tau_c}{h} \quad (11)$$

which is the inverse of the Damköhler number calculated at the height of the canopy top,  $h$ . Thus we introduce canopy-top Damköhler number as

$$Da_h = \frac{1}{\tau_c^N} = \frac{h}{u_* \tau_c}. \quad (12)$$

Damköhler number for a specific measurement height can be obtained from this by

$$Da = z_n Da_h \quad (13)$$

where  $z_n$  is the measurement height normalized with canopy height ( $z_n = z/h$ ).

### 3 Measurements of oxidants during HUMPPA – COPEC – 2010

The measurements of oxidants used to calculate the chemical lifetimes of VOCs were conducted at SMEAR II research station in Hyytiälä, Finland as part of the HUMPPA-COPEC-2010 measurement campaign. A detailed description of the measurement campaign has been given by Williams et al. (2011) while the measurement station has been described by Hari and Kulmala (2005). Below we give a short description of the measurements utilized in this study.

#### 3.1 Hydroxyl radical concentration

Our measurement of hydroxyl radical (OH) relies on the detection of isotopically labeled sulfuric acid with the Chemical Ionization Mass Spectrometer (CIMS). This technique is discussed by Eisele and Tanner (1991, 1993), Tanner et al. (1997), and Petäjä et al. (2009) in more detail. An important note on the method that needs to be kept in mind is that we do not measure OH directly, but only infer the ambient OH concentration looking into how much of the isotopically labeled  $^{34}\text{SO}_2$  is converted to isotopically labeled sulfuric acid with a constant reaction time. During the HUMPPA-COPEC campaign (Williams et al. 2011) we compared the CIMS method with a Laser induced fluorescence (LiF) detection of OH (Faloona et al. 2004) and the agreement was excellent, with a slope of 1.05 based on side-by-side measurements (H. Harder, personal communication, 2011).

#### 3.2 Nitrate radical concentration

Nitrate radical ( $\text{NO}_3$ ) was measured at night by cavity-ring-down spectroscopy using the setup described in Crowley et al. (2010). Typically, measurements were commenced 1–2 h

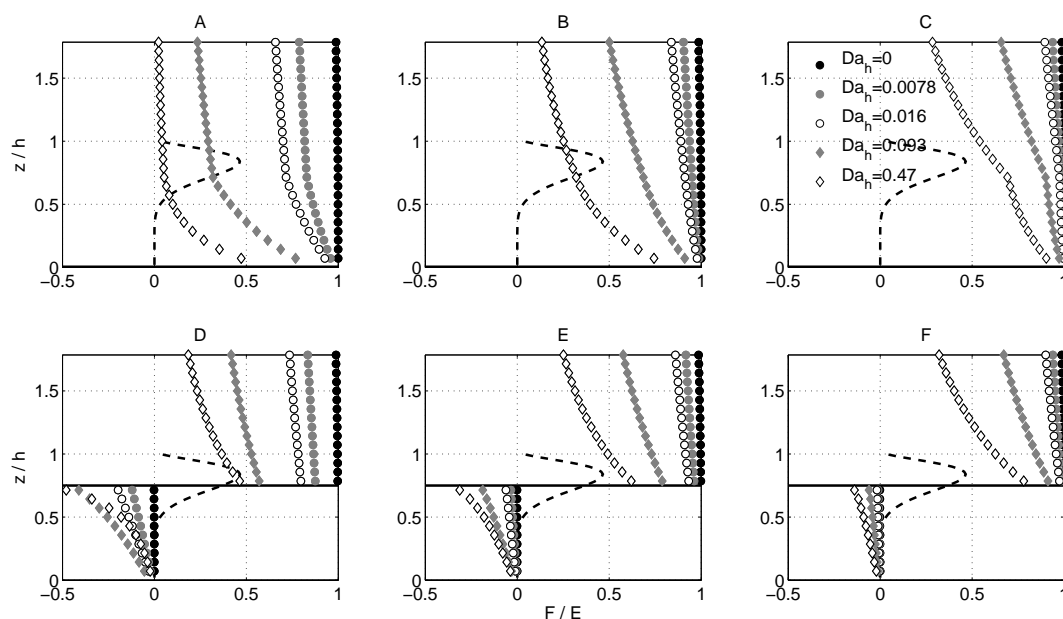


**Fig. 2.** Flux-to-surface-exchange ( $F/E$ ) ratio profiles. The source height, represented by the solid black line, is at the ground level in Panels (A)–(C) and at the displacement height in Panels (D)–(F). In Panels (B) and (E) the vertical profile of oxidation rate is constant. In Panels (A) and (D) the oxidation rate below the displacement height is four times faster than above that. In Panels (C) and (F) the oxidation rate below displacement height is one-fourth of that above displacement height. The canopy-top Damköhler refers to the above canopy chemical lifetime in all Panels. The dashed black line represents the foliage distribution.

before sunset, around 23:00 LT, and stopped 1 h after sunrise, around 04:00 LT. The two-channel instrument, which sampled  $\text{NO}_3$  and the sum of  $\text{NO}_3$  plus  $\text{N}_2\text{O}_5$  was located at the top of a  $\sim 20$  m tower, i.e. approximately at canopy height. The horizontal distance to the nearest tree-top was about 10 meters. The accuracy of the measurements, considering errors in the cross sections of  $\text{NO}_3$ , inlet and filter losses of  $\text{NO}_3$  and variability in the zero measurements, was about 20 %, with a limit of detection of about 1 pptv ( $2 \times 10^7$  molecule  $\text{cm}^{-3}$ ). During the entire campaign both  $\text{NO}_3$  and  $\text{N}_2\text{O}_5$  were below the detection limit. The low  $\text{NO}_3$  mixing ratios were a result of a low  $\text{NO}_3$  production term, average nighttime  $\text{NO}_2$  and  $\text{O}_3$  being about 350 pptv and 40 ppbv, respectively, resulting in an average  $\text{NO}_3$  production rate of  $1 \times 10^{-2}$  pptv  $\text{s}^{-1}$ . The average loss rate for  $\text{NO}_3$  due to reaction with  $\alpha$ -pinene,  $\beta$ -pinene and 3-carene was about  $0.03 \text{ s}^{-1}$  with approximate maximum and minimum values on individual nights of  $0.07 \text{ s}^{-1}$  and  $0.01 \text{ s}^{-1}$ , respectively. When combined with the lowest nighttime reactivity ( $1 \times 10^2 \text{ s}^{-1}$ ) this results in a steady state  $\text{NO}_3$  mixing ratio of 1 pptv only.

### 3.3 Ozone concentration

Ozone ( $\text{O}_3$ ) was measured during HUMPPA COPEC-2010 campaign from the 73 m mast of the SMEAR II at different heights. For characteristic values, mean values of 30 min averages at 16.8 m height were used in the study. The  $\text{O}_3$  mix-

ing ratio was determined using a Thermo Environment model TEI-49 instrument relying on ultra-violet absorption.

## 4 Results and discussion

### 4.1 Oxidation profile and emission height

Figure 2 represents flux-to-surface-exchange ratio ( $F/E$ ) profiles in hydrostatically neutral stratification, for canopy density and shape representing a typical Scots pine forest. In middle panels (b and e) the chemical lifetime is vertically constant representing a constant profile of oxidation rate while the left side panels (a and d) represent the case where the oxidation rate below canopy is four times faster than above the canopy. This could be due to e.g. higher  $\text{NO}_3$  concentrations in the shaded canopy environment (Forkel et al., 2006). In the right side panels (c and f) the chemical lifetime below the displacement height is four times longer, corresponding e.g. to a case where the OH level in shaded below-canopy environment is lower than above canopy. This type of OH profile was also experimentally observed.

The vertical profile of the chemical lifetime shows the expected influence on the  $F/E$  profile in the cases with source height at ground level (Fig. 2, panels a–c), but also affects the above canopy  $F/E$  profiles of the cases with source at the displacement height (Fig. 2, panels d–f). Because part of the trajectories, starting from the canopy, move below source height before being transported upwards, they are influenced

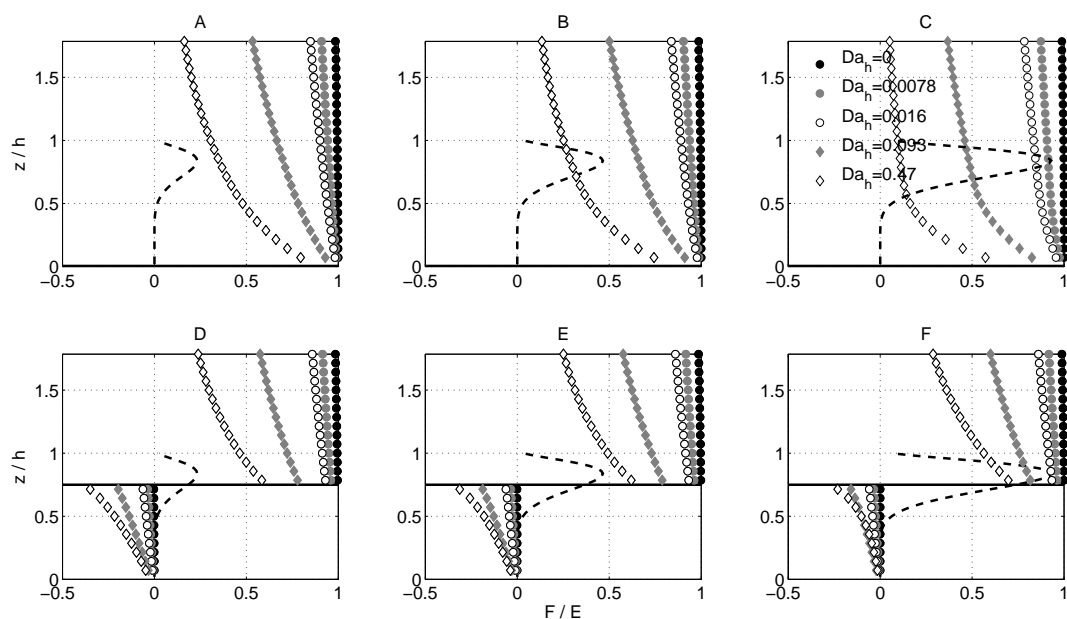


**Fig. 3.** Effect of canopy density on flux-to-surface-exchange ( $F/E$ ) ratio. The source height, represented by the solid black line, is at the ground level in Panels (A)–(C) and at the displacement height in Panels (D)–(F). In Panels (B) and (E) the canopy density corresponds to that in SMEAR II and used also in Fig. 2. In Panels (A) and (D) the canopy density is half of that in Panels (B) and (E), and in Panels (C) and (F) the canopy density is double of that in Panels (B) and (E). The canopy-top Damköhler refers to the above canopy chemical lifetime in all Panels. The dashed black line represents the foliage distribution.

by the oxidant levels also below the source level. In panels d–f we can observe negative  $F/E$  values for chemically reactive cases below the source height, due to the downward fluxes caused by the chemical sink. In the end the oxidation rates below source level do have an effect on the above canopy fluxes as the air parcels, which have traveled below source level prior to crossing the observation level above the canopy, have been exposed to the oxidant level below the source level.

The  $F/E$  profiles obtained (Fig. 2) are similar as the ones presented earlier by Rinne et al. (2007). However, whereas they presented their results for a specific friction velocity and canopy height we present them in normalized, dimensionless forms as calculated by the SLTC model and show the chemical lifetime as Damköhler number at the canopy-top ( $Da_h$ ), as given by Eq. (12). Heights above the surface are relative to the canopy height. This will enable a wider utilization of these results. As the model scales linearly with the friction velocity, one can obtain chemical lifetimes using Eq. (12). If, for example, we consider a compound with chemical lifetime of 30 minutes emitted from the forest canopy with a height of 18 m and the friction velocity is  $0.5 \text{ m s}^{-1}$ , the canopy-top Damköhler number is 0.02. If the flux measurement height is 22 m the corresponding Damköhler number is 0.024. From Figure 2 we can observe that the fluxes above canopy are significantly reduced already at Damköhler numbers well below unity. For example in the case of vertically constant chemical lifetime and source at the displacement

height (panel e) the flux at the measurement height of 1.5 times the canopy height ( $h$ ) is reduced by 12 % at Damköhler number, calculated for  $z = 1.5 \times h$ , of 0.026, and 38 % at Damköhler number of 0.14. One reason for this is the definition of mixing time scale (Eq. 6) we used in the Damköhler number. The transport times inside the canopy are not well characterized by this formulation. The mixing time-scale calculated with this formula for measurement height of 22.5 m ( $z_m = 1.5 \times h$ ,  $h = 15 \text{ m}$ ) and  $u^* = 1 \text{ m s}^{-1}$  is 22.5 s. We can also calculate average transport times using our model by registering the time difference from release of air-parcel to the crossings of observation level, and averaging these. This approach yields transport time for air parcels originating from the canopy ( $z_m = 1.5 \times h$ ,  $h = 15 \text{ m}$ ,  $u^* = 1 \text{ m s}^{-1}$ ) of 42 s in the case only the first crossing was considered and 310 s when all crossings were taken into account. Alternatively we can invert the Eq. (9) and calculate the effective transport time from the  $F/E$  ratios for constant oxidant profiles (Fig. 3). This approach gives effective transport times for parcels originating from canopy between 57 s and 150 s depending on the reactivity. The shortest effective transport times are obtained using the case with highest  $Da_h$ . The differences in the transport times given by different methods can be explained by the implicitly different definitions for the transport time. The effective transport time calculated by inverted Eq. (9) weighs subsequent crossings differently depending on the reactivity. The shorter the lifetime, more

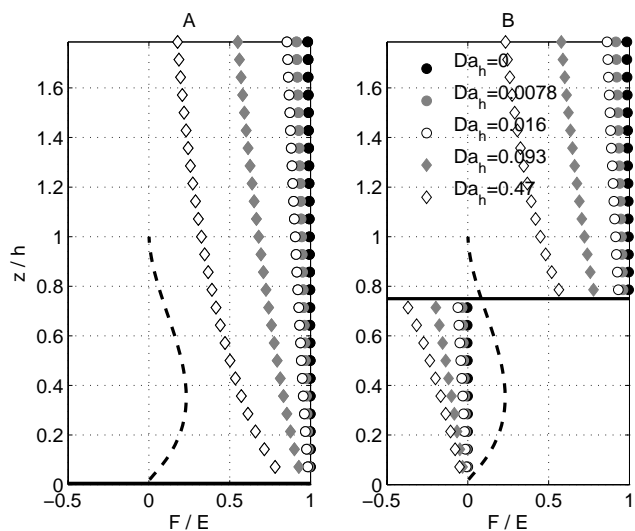


**Fig. 4.** The flux-to-surface-exchange ( $F/E$ ) ratio profiles calculated using foliage distribution (dashed black line) typical for spruce forest. The vertical profile of oxidation rate is constant and the source is either at the ground level (Panel A) or at the height corresponding to the displacement height of the Scots pine forest.

weight the first crossing gets compared to the later ones, leading to shorter effective transport time.

#### 4.2 Canopy density and structure

The canopy can increase the chemical loss by hindering transport and thus prolonging the transport time, in addition to affecting the lifetimes of VOCs by influencing the concentrations of oxidants. Keeping the vertical oxidation profile constant we investigated the effect of (i) halving or doubling canopy density of a Scots pine type forest at SMEAR II (Fig. 3) and (ii) changing the canopy shape from Scots pine to spruce (Fig. 4). The canopy density exerts the expected influence on the  $F/E$  profiles in the case with the source at the ground level. The increase in the canopy density reduces the turbulence below the canopy and thus the transport time from the ground source to above canopy levels increase. This leads to increased flux degradation above the canopy, as there is more time for oxidation. Interestingly, the  $F/E$  profile in the case with the source at the displacement height seems to be rather insensitive to the canopy density. Obviously the increase in the canopy density reduces the transport downwards from the source level as well as upwards transport. Thus it seems that these two effects counterbalance each other and the net effect of canopy density to the  $F/E$  profiles when the source is at the displacement height is minimal. We must remind here that in this modeling exercise the oxidant profiles were kept constant in spite of changes in canopy density. In reality the increase in canopy density would be likely to reduce the below canopy levels of OH and ozone through shading and providing more surface to deposition. Thus in-

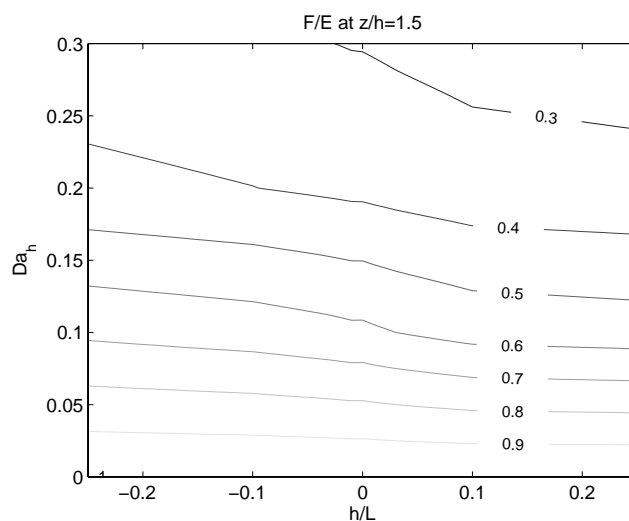


**Fig. 5.** Effect of stability on the flux-to-surface-exchange ( $F/E$ ) ratio at the height where measurement height ( $z$ ) ratio to the canopy height ( $h$ ) is 1.5. On x-axis is the inverse of the Obukhov length ( $L$ ) normalized with canopy height ( $h$ ) and on y-axis is the canopy-top Damköhler number. The numbers on curves refer to flux-to-emission ratios.

creased canopy density may even increase the above-canopy  $F/E$  ratio for reactive compounds emitted from the canopy.

The  $F/E$  profiles for spruce forest (Fig. 4) are quite similar than for the canopy structure of pine forest (Fig. 3, panel b and e). However, as we choose to have the canopy source at the same height as in the case for Scots pine to ease the comparison between these two, this emission height may be somewhat artificial as for spruce most of the needle biomass is at lower height.

By using the  $F/E$  profiles shown in Fig. 2, 3 and 4 we can assess the importance of below canopy chemical processing to the above canopy one. The degradation below and within canopy is given by  $1 - F/E(h)$  whereas the degradation between canopy top and measurement height is given as  $F/E(h) - F/E(z_m)$ . If we set the measurement height to  $1.5 \times h$ , which is a typical flux measurement height, we see that from 50 % up to over 90 % of the chemical degradation occurs within and below canopy. Even when the source is within the canopy 50 % to well over 80 % of the degradation can occur within and below canopy.

#### 4.3 Hydrostatic stability

All the results discussed above are calculated for hydrostatically neutral stratification. In Fig. 5 the effect of stratification on the  $F/E$  values at the height of  $1.5h$  is represented. The stability is presented as Obukhov length

$$L = - \frac{u^*{}^3 \overline{\theta_v}}{\kappa g (\overline{w'\theta_v})_s} \quad (14)$$

where  $\theta_v$  is virtual potential temperature,  $\kappa$  is von Kármán constant, and subscript *s* refers to surface value (Obukhov, 1971), normalized with canopy height ( $h/L$ ). The stability range in the figure ( $-0.25 < h/L < 0.25$ ) ranges from moderately unstable to moderately stable, as an example for canopy height of 15 m from  $L = -60$  m to  $L = 60$  m. Not surprisingly, the normalized fluxes for a given normalized chemical lifetimes are lower in the stable than in the unstable stratification. However, the direct effect of the stability is small compared to that of  $Da_h$ , i.e. friction velocity and chemical lifetime. If, for example we consider a compound with chemical lifetime corresponding to top-of-the-canopy Damköhler number of 0.1 we find that the flux is reduced by 38 % in neutral case, 32 % when  $h/L = -0.25$  (for  $h = 15$  m,  $L = -60$ ) and 45 % when  $h/L = 0.25$ , when all other parameters, including friction velocity are kept constant. We can see from Eq. (14) that this implies that only buoyancy flux is varying in this case. However, as in reality stability exerts a strong control on the turbulence, it has an indirect effect on the flux profiles via the friction velocity.

One must note that in reality, especially in dense canopies, the stability below the canopy can be the opposite to the stability above the canopy. This can greatly modify the transport times inside the canopy and can have a strong effect especially on the  $F/E$  ratios of those compounds emitted from forest floor.

If we neglect the direct effect of stability, to a first approximation, we can draw a relation between flux degradation at certain height, friction velocity, and chemical lifetime of a compound. In Fig. 6 is an example for such a relation for source of reactive compound in the canopy and constant oxidation rate profile. The x-axis shows the top-of-the-canopy Damköhler number, function of friction velocity and chemical lifetime, and the y-axis the height normalized by dividing with the canopy height. The isolines indicate  $F/E$  values determined from profiles shown in Fig. 2, panel e by interpolation. We have derived these for normalized chemical lifetime ranges we have the original SLTC runs for and for all the pine canopy densities and oxidation rate profiles (Supplementary material).

#### 4.4 Case study: BVOC fluxes and HUMPPA-COPEC-2010 oxidant measurements

Using the data used to generate Fig. 6 as a lookup table we can assess the importance of the chemical degradation in different conditions. As an example we chose three compounds typically emitted by boreal forests. First one is isoprene, the globally dominant biogenic volatile organic compound (Guenther et al., 1995); the second is  $\alpha$ -pinene, the dominant monoterpene in the ecosystem scale emission from Scots pine forests such as Hyytiälä (Rinne et al., 2000; Räisänen et al., 2009). These two have typical daytime atmospheric lifetimes of about half an hour in summertime conditions in Hyytiälä. The third compound is  $\beta$ -caryophyllene, a typical

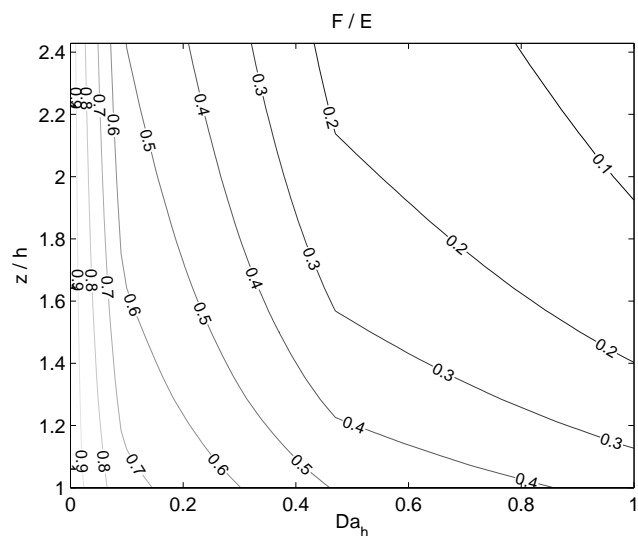


**Fig. 6.** Flux-to-surface-exchange ( $F/E$ ) ratio as a function of canopy-top Damköhler number and ratio of measurement height ( $z$ ) to the canopy height ( $h$ ). This is a visualization of the look-up table (Supplementary material).

sesquiterpene compound emitted by pine trees (e.g. Hakola et al., 2006). It is more reactive than isoprene or  $\alpha$ -pinene with a daytime lifetime in summertime Hyytiälä conditions below two minutes. By using typical diurnal cycles of the three oxidants and friction velocity (Fig. 7) and their reaction rate constants (Table 2) we can calculate the diurnal cycle of each compounds lifetime (Eq. 4). The diurnal cycles of friction velocity, ozone and hydroxyl radical concentrations are hourly medians measured during HUMPPA-COPEC-2010 campaign (Williams et al., 2011) conducted in SMEAR II research station (Hari and Kulmala, 2005) in July-August 2010, as described above. The effect of stability was ignored for simplicity. During the HUMPPA-COPEC-2010 the daytime median  $h/L = -0.1$  and night time median  $h/L = 0.25$ . Also nitrate radical concentrations were measured; however, since they were below detection limit we used calculated value of  $2.5 \times 10^7$  molecules  $\text{cm}^{-3}$  (1 pptv) at night (22:00–04:00) and zero during daytime.

The relative importance of the three oxidants in the chemical degradation on the three VOCs at hand can be seen in Table 3, in which we present oxidative capacities,  $R$ , of the three oxidants against VOCs. The oxidative capacities are calculated as

$$R_{\text{ox}}^X = k_{X,\text{ox}} [\text{ox}] \quad (15)$$

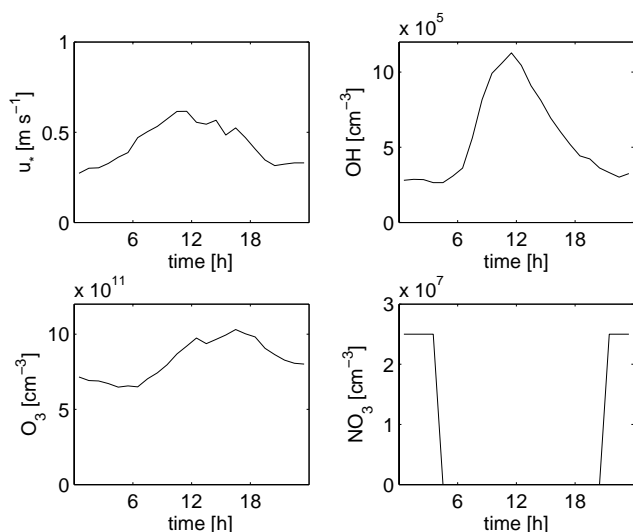
where sub- and superscript  $X$  refers to VOC (in this case isoprene,  $\alpha$ -pinene or  $\beta$ -caryophyllene), ox to oxidant (ozone, hydroxyl radical, or nitrate radical), and  $[\text{ox}]$  is the oxidant concentration. No oxidant has an overwhelming importance on the oxidation of all the three VOCs. Instead their relative importance varies case to case. Two striking results emerge

**Table 2.** Reaction coefficients of isoprene,  $\alpha$ -pinene and  $\beta$ -caryophyllene against OH, O<sub>3</sub> and NO<sub>3</sub>. Reaction coefficients for isoprene and  $\alpha$ -pinene from Atkinson (1994) and those for  $\beta$ -caryophyllene from Shu and Atkinson (1995).

	OH cm <sup>3</sup> molecule <sup>-1</sup> s <sup>-1</sup>	O <sub>3</sub> cm <sup>3</sup> molecule <sup>-1</sup> s <sup>-1</sup>	NO <sub>3</sub> cm <sup>3</sup> molecule <sup>-1</sup> s <sup>-1</sup>
isoprene	$10.1 \times 10^{-11}$	$1.28 \times 10^{-17}$	$6.78 \times 10^{-13}$
$\alpha$ -pinene	$5.37 \times 10^{-11}$	$8.66 \times 10^{-17}$	$6.16 \times 10^{-12}$
$\beta$ -caryophyllene	$2.00 \times 10^{-10}$	$1.16 \times 10^{-14}$	$1.90 \times 10^{-11}$

**Table 3.** Oxidative capacities of OH, O<sub>3</sub> and NO<sub>3</sub> to isoprene,  $\alpha$ -pinene, and  $\beta$ -caryophyllene.  $\Delta\%$  is the proportion to the uncertainty to the total oxidative capacity of given VOC.

Day	$R_{OH}$ , s <sup>-1</sup>	$\Delta\%$	$R_{O_3}$ , s <sup>-1</sup>	$\Delta\%$	$R_{NO_3}$ , s <sup>-1</sup>	$\Delta\%$	$R_{Total}$
	Isoprene	$1.1 \pm 0.4 \times 10^{-4}$	36	$1.21 \pm 0.03 \times 10^{-5}$	0.3	0	–
$\alpha$ -pinene	$6 \pm 2 \times 10^{-5}$	17	$8.2 \pm 0.2 \times 10^{-5}$	2	0	–	$1.4 \pm 0.2 \times 10^{-4}$
$\beta$ -caryophyllene	$2.2 \pm 0.9 \times 10^{-4}$	0.8	$1.10 \pm 0.03 \times 10^{-2}$	3	0	–	$1.1 \pm 0.3 \times 10^{-2}$
Night							
Isoprene	$3 \pm 1 \times 10^{-5}$	21	$9.9 \pm 0.3 \times 10^{-6}$	0.6	$1.7 \pm 1.7 \times 10^{-5}$	30	$7 \pm 2 \times 10^{-5}$
$\alpha$ -pinene	$1.5 \pm 0.6 \times 10^{-5}$	2	$6.7 \pm 0.2 \times 10^{-5}$	0.9	$1.7 \pm 1.7 \times 10^{-4}$	67	$2.5 \pm 1.6 \times 10^{-4}$
$\beta$ -caryophyllene	$6 \pm 2 \times 10^{-5}$	0.2	$9.0 \pm 0.3 \times 10^{-3}$	3	$5 \pm 5 \times 10^{-4}$	5	$9.5 \pm 0.6 \times 10^{-3}$

**Fig. 7.** Typical diurnal cycles of friction velocity, OH, O<sub>3</sub>, and NO<sub>3</sub>, as derived from measurements during HUMPPA-COPEC-2010 campaign.

from the table. First, even at these low calculated nighttime NO<sub>3</sub> levels the nitrate radical dominates the  $\alpha$ -pinene oxidation at night. Second, the low observed levels of OH at night are still sufficient to account for a half of nighttime isoprene oxidation. Also presented in the Table 3 are the estimated uncertainties of oxidative capacities due to the uncertainties of oxidant measurements ( $\Delta O_3 = 1$  ppb,  $\Delta OH = 40\%$ ,  $\Delta NO_3 = 1$  ppt). We can see from the Table 3 that largest un-

certainties arise from the uncertainties of OH in the case of daytime isoprene oxidation and NO<sub>3</sub> in the case of nighttime  $\alpha$ -pinene oxidation

In order to use the look-up table (see Supplement) we calculated the diurnal cycle of the canopy-top Damköhler number ( $Da_h$ ) for each VOC by using the diurnal cycle of their chemical lifetime (Eq. 4), the diurnal cycle of the friction velocity, and Eq. (11). The canopy height was set to 18 m. The flux-to-emission ratio was then retrieved from the look-up table for VOC flux measurement height used in SMEAR II (22 m =  $1.2 \times h$ ).

The resulting flux to emission ratios, for both source in the ground (upper panel) and in the canopy (lower panel) are shown in Fig. 8. One can see that the  $F/E$  ratio of isoprene is close to unity throughout the diurnal cycle for both source heights, implying that the fluxes above the canopy closely correspond to the emission. Furthermore, there is very little diurnal cycle in the  $F/E$  ratio and thus the functional relations between the emission and environmental parameters will be reflected to the fluxes. The  $F/E$  ratio of  $\alpha$ -pinene is close to unity during daytime, but falls to values below 0.9 during night. This affects the total daily emission only a little, especially as the emission during nighttime are smaller than during the daytime. However, the chemical degradation can have an effect on functional relations between monoterpene emission and environmental parameters, derived using above canopy fluxes. This is due to the environmental parameters affecting the terpenoid emission, such as temperature and light, having similar diurnal cycles than the flux-to-emission ratio. In order to investigate the effect, we

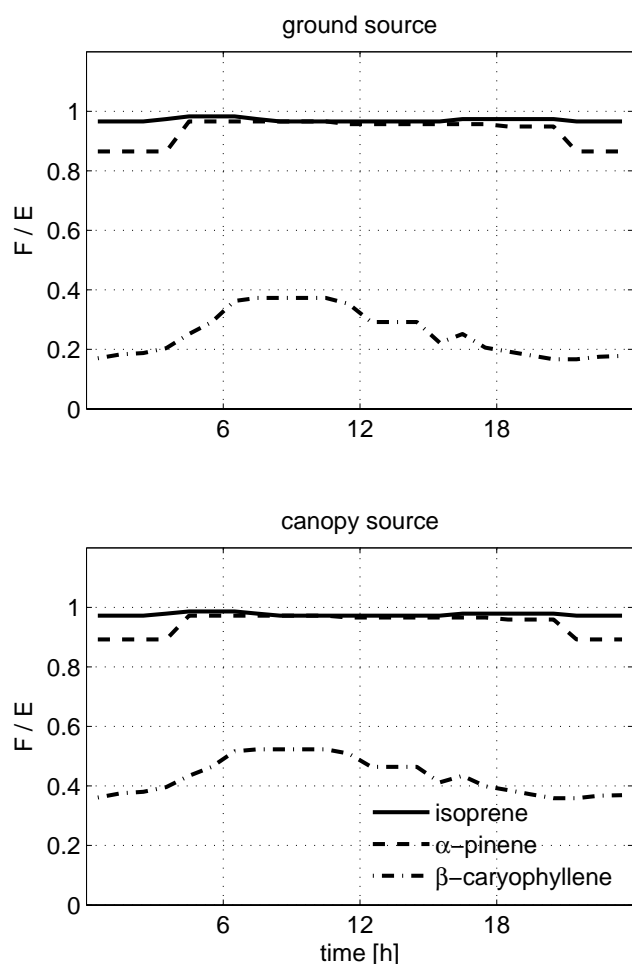


**Fig. 8.** Diurnal cycle of the flux-to-surface-exchange ( $F/E$ ) ratios of isoprene,  $\alpha$ -pinene and  $\beta$ -caryophyllene for conditions during HUMPPA-COPEC-2010 campaign.

calculated the  $\alpha$ -pinene emissions using median diurnal cycle of temperatures observed during HUMPPA-COPEC campaign with emission algorithm by Guenther et al. (1993)

$$E = E_{30} \exp(\beta (T - 30^\circ\text{C})) \quad (16)$$

where  $E_{30}$  is the emission standardized to  $30^\circ\text{C}$  temperature,  $\beta$  is the temperature sensitivity of the emission, and  $T$  is the temperature. For temperature sensitivity of monoterpenes we used value of  $\beta = 0.09^\circ\text{C}^{-1}$ . After emission calculated for each hour was multiplied by corresponding  $F/E$  ratio we fitted the temperature against flux obtained to yield the  $\beta$  value for the flux. The temperature dependence obtained from the fluxes was  $\beta = 0.098^\circ\text{C}^{-1}$  and  $\beta = 0.100^\circ\text{C}^{-1}$  for canopy and ground source, respectively. Thus a slightly steeper temperature dependence of fluxes than that of primary emission is observed

The chemical degradation affects the fluxes of  $\beta$ -caryophyllene even more as its  $F/E$  ratio is below 0.4 for ground source and about 0.5 for canopy source during the

daytime and falls below 0.2 for ground source and below 0.4 for canopy source during night. Thus the emission of this highly reactive compound is seriously underestimated by the above canopy fluxes. If we use Eq. (16) with  $\beta = 0.18^\circ\text{C}^{-1}$  (Hakola et al., 2006) to calculate the surface emission of  $\beta$ -caryophyllene, the temperature dependence of fluxes becomes  $\beta = 0.19^\circ\text{C}^{-1}$  and  $\beta = 0.20^\circ\text{C}^{-1}$  for canopy and ground source, respectively. As the current development in online mass spectrometry enables the flux measurements of the highly reactive sesquiterpenes (Müller et al., 2010; Ruuskanen et al., 2011) it is of great importance to better understand the processes linking the measured above canopy fluxes to the primary emission of reactive compounds.

## 5 Conclusions

We have used a stochastic Lagrangian transport model with simplified chemical degradation to estimate the effect of chemistry on ratio of the above canopy fluxes and primary emission. The flux degradation was mostly dependent on the chemical lifetime of the compound and on the friction velocity as the Damköhler number depends on these parameters. Stability as given by the Obukhov-length had a smaller direct effect but it affects the flux-to-surface-exchange ( $F/E$ ) ratio also via its effect on turbulence intensity. The degradation was stronger for emission from the ground level than from the emission from the canopy, due to longer time required for transport to the above canopy atmosphere.

The oxidant profile had a significant effect on the  $F/E$  ratio. In the case with higher oxidation rate below canopy the fluxes were degraded more than in the case with constant oxidation rate. This was case also when the reactive compound was emitted from the canopy. As 50% or more of the flux degradation occurs below the canopy, the better characterization of the below-canopy turbulent transport and oxidant profiles is essential for understanding the fluxes of reactive compounds. The canopy density had a significant effect only when the emission occurred in the ground level.

We used the results from simulations to create a look-up table relating the chemical lifetime of a compound, friction velocity and the resulting flux to emission ratio. This look-up table was used with turbulence and oxidant data measured during HUMPPA-COPEC-2010 field campaign to estimate the effect of chemical degradation on the fluxes of three biogenic hydrocarbons, isoprene,  $\alpha$ -pinene, and  $\beta$ -caryophyllene. For isoprene the effect of the chemical degradation on flux to emission ratio was a minor one. The flux to emission ratio of  $\alpha$ -pinene was moderately affected while for  $\beta$ -caryophyllene the chemical degradation had a major effect. Furthermore, if the daily cycle of flux-to-emission ratio is not taken into account it may distort the interpreted dependencies of emission on environmental parameters. As the diurnal cycle of the flux-to-emission ratio follows the course of diurnal cycles of e.g. solar radiation and air temperature,

interpreting flux directly as emission can lead to artificial correlations between emission and these environmental parameters.

There are uncertainties of the various parts of the approach. Many of these have to do with the below-canopy atmosphere. First the below canopy turbulent flow is not well characterized as shown by reported discrepancies between observations and models. Also the basal layer, as the soil emissions must traverse it, should be better characterized. While ozone concentration profiles within and below many plant canopies have been measured, the profiles or even above and below canopy concentrations of hydroxyl and nitrate radical are often lacking. Furthermore the so-called segregation effect, which can affect the calculated chemical life times, is hardly well known. These all call for further studies of the interactions between chemistry and turbulent transport above and within plant canopies.

**Supplementary material related to this article is available online at:** <http://www.atmos-chem-phys.net/12/4843/2012/acp-12-4843-2012-supplement.zip>.

*Acknowledgements.* Funding from the Academy of Finland (139656, 1118615, 120434, 125238), Finnish Centre of Excellence funded by Academy of Finland (141135), and European Research Council (227463-ATMNUCLE) is gratefully acknowledged. Help of the SMEAR II personnel (J. Levula, T. Pohja, V. Hiltunen, H. Laakso) during the field campaign is gratefully acknowledged.

Edited by: D. Heard

## References

- Atkinson, R.: Gas-phase tropospheric chemistry of organic compounds, *J. Phys. Chem. Ref. Data. Monogr.*, 2, 216 pp., 1994.
- Boy, M., Sogachev, A., Lauros, J., Zhou, L., Guenther, A., and Smolander, S.: SOSA – a new model to simulate the concentrations of organic vapours and sulphuric acid inside the ABL – Part I: Model description and initial evaluation, *Atmos. Chem. Phys.*, 11, 43–51, doi:10.5194/acp-11-43-2011, 2011.
- Ciccioli, P., Brancaleoni, E., Frattoni, M., Di Palo, V., Valentini, R., Tirone, G., Seufert, G., Bertin, N., Hansen, U., Csiky, O., Lenz, R., and Sharma, M.: Emission of reactive terpene compounds from orange orchards and their removal by within-canopy processes. *J. Geophys. Res.*, 104, 8077–8094, 1999
- Crowley, J.N., Schuster, G., Pouvesle, N., Parchatka, U., Fischer, H., Bonn, B., Bingemer, H., and Lelieveld, J.: Nocturnal nitrogen oxides at a rural mountain site in south-western Germany, *Atmos. Chem. Phys.*, 10, 2795–2812, doi:10.5194/acp-10-2795-2010, 2010.
- Damköhler, G.: Der Einfluss der Turbulenz auf die Flammgeschwindigkeit in Gasgemischen, *Zeitschrift für Electrochemie und Angewandte Physikalische Chemie*, 46, 601–626, 1940.
- Eisele, F. and Tanner, D.: Ion-assisted tropospheric OH measurements, *J. Geophys. Res.*, 96, 9295–9308, 1991.
- Eisele, F. and Tanner, D.: Measurement of the gas phase concentration of H<sub>2</sub>SO<sub>4</sub> and methane sulfonic acid and estimates of H<sub>2</sub>SO<sub>4</sub> production and loss in the atmosphere, *J. Geophys. Res.*, 98, 9001–9010, 1993.
- Faloona, I. C., Tan, D., Leshner, R. L., Hazen, N. L., Frame, C. L., Simpas, J. B., Harder, H., Martinez, M., Di Carlo, P., Ren, X., and Brune, W. H.: A Laser-induced Fluorescence Instrument for detecting tropospheric OH and HO<sub>2</sub>: characteristics and calibration, *J. Atmos. Chem.* 47, 139–167, 2004
- Forkel, R., Klemm, O., Graus, M., Rappengluck, B., Stockwell, W. R., Grabmer, W., Held, A., Hansel, A., and Steinbrecher, R.: Trace gas exchange and gas phase chemistry in a Norway spruce forest: A study with a coupled 1-dimensional canopy atmospheric chemistry emission model, *Atmos. Environ.*, 40, Supplement 1, S28–S42, 2006.
- Fowler, D., Pilegaard, K., Sutton, M. A., Ambus, P., Raivonen, M., Duyzer, J., Simpson, D., Fagerli, H., Fuzzi, S., Schjoerring, J. K., Granier, C., Nefel, A., Isaksen, I. S. A., Laj, P., Maione, M., Monks, P. S., Burkhardt, J., Daemmgen, U., Neirynek, J., Personne, E., Wichink-Kruit, R., Butterbach-Bahl, K., Flechard, C., Tuovinen, J. P., Coyle, M., Gerosa, G., Loubet, B., Altimir, N., Gruenhage, L., Ammann, C., Cieslik, S., Paoletti, E., Mikkelsen, T. N., Ro-Poulsen, H., Cellier, P., Cape, J. N., Horváth, L., Loreto, F., Niinemets, Ü., Palmer, P. I., Rinne, J., Misztal, P., Nemitz, E., Nilsson, D., Pryor, S., Gallagher, M. W., Vesala, T., Skiba, U., Brüeggemann, N., Zechmeister-Boltenstern, S., Williams, J., O'Dowd, C., Facchini, M. C., de Leeuw, G., Flossman, A., Chaumerliaco, N., and Erisman, J. W.: Atmospheric Composition Change: Ecosystems – Atmosphere interactions. *Atmos. Environ.*, 43, 5193–5267, 2009
- Guenther, A., Zimmermann, P., Harley, P., Monson, R., and Fall, R.: Isoprene and monoterpene emission rate variability: Model evaluation and sensitivity analysis, *J. Geophys. Res.*, 98, 12609–12617, 1993.
- Guenther, A., Hewitt, C. N., Erickson, D., Fall, R., Geron, C., Graedel, T., Harley, P., Klinger, L., Lerdau, M., McKay W. A., Pierce T., Scholes, B., Steinbrecher, R., Tallamraju, R., Taylor, J., and Zimmerman, P.: A global model of natural volatile organic compound emissions. *J. Geophys. Res.*, 100, 8873–8892, 1995
- Hakola, H., Tarvainen, V., Bäck, J., Ranta, H., Bonn, B., Rinne, J., and Kulmala, M.: Seasonal variation of mono- and sesquiterpene emission rates of Scots pine. *Biogeosci.*, 3, 93–101, 2006.
- Hari, P. and Kulmala, M.: Station for measuring ecosystem atmosphere relations (SMEAR II), *Boreal Environ. Res.*, 10, 315–322, 2005.
- Hörtnagl, L., Bamberger, I., Graus, M., Ruuskanen, T. M., Schnitzhofer, R., Müller, M., Hansel, A., and Wohlfahrt G.: Biotic, abiotic, and management controls on methanol exchange above a temperate mountain grassland, *J. Geophys. Res.*, 116, G03021, doi:10.1029/2011JG001641, 2011.
- Kesselmeier, J., Guenther, A., Hoffmann, T., Piedade, M. T., and Warnke, J.: Natural volatile organic compound emissions from plants and their roles in oxidant balance and particle formation, in: Amazonia and global change, edited by: Keller, M., Bustamante, M., Gash, J. H. C., and Silva Dias, P., *Geophysical Monograph*, American Geophysical Union, Washington DC,

- USA, 183–206, 2009.
- Launiainen, S., Rinne, J., Pumpanen, J., Kulmala, L., Kolari, P., Keronen, P., Siivola, E., Pohja, T., Hari, P., and Vesala, T.: Eddy-covariance measurements of CO<sub>2</sub> and sensible and latent heat fluxes during a full year in a boreal pine forest trunk-space. *Boreal Environ. Res.*, 10, 569–588, 2005
- Markkanen, T., Rannik, Ü., Marcolla, B., Cescatti, A. and Vesala, T.: Footprints and fetches for fluxes over forest canopies with varying structure and density, *Bound.-Layer Meteorol.*, 106, 437–459, 2003.
- Massman, W. J.: An Analytical one-dimensional model of momentum transfer by vegetation of arbitrary structure, *Bound.-Layer Meteorol.*, 83, 407–421, 1997.
- Massman, W. J. and Weil, J. C.: An analytical one-dimensional second-order closure model of turbulence statistics and the Lagrangian time scale within and above plant canopies of arbitrary structure, *Bound.-Layer Meteorol.* 91, 81–107, 1999.
- Müller, M., Graus, M., Ruuskanen, T. M., Schnitzhofer, R., Bamberger, I., Kaser, L., Titzmann, T., Hörtnagl, L., Wohlfahrt, G., Karl, T., and Hansel, A.: First eddy covariance flux measurements by PTR-TOF, *Atmos. Meas. Tech.*, 3, 387–395, doi:10.5194/amt-3-387-2010, 2010.
- Obukhov, A. M.: Turbulence in an atmosphere with a non-uniform temperature. *Bound.-Layer Meteorol.* 2, 7–29, 1971
- Petäjä, T., Mauldin III, R. L., Kosciuch, E., McGrath, J., Nieminen, T., Adamov, A., Kotiaho, T., and Kulmala, M.: Sulfuric acid and OH concentrations in a boreal forest site, *Atmos. Chem. Phys.* 9, 7435–7448, doi:10.5194/acp-9-7435-2009, 2009
- Räisänen, T., Ryyppö, A., and Kellomäki, S.: Monoterpene emission of a boreal Scots pine (*Pinus sylvestris* L.) forest, *Agric. For. Meteorol.*, 149, 808–819, 2009.
- Rannik, Ü., Aubinet, M., Kurbanmuradov, O., Sabelfeld, K. K., Markkanen, T., and Vesala, T.: Footprint analysis for measurements over a heterogeneous forest. *Bound.-Layer Meteorol.*, 97, 137–166, 2001.
- Rannik, Ü., Markkanen, T., Raittila, J., Hari, P., and Vesala, T.: Turbulence statistics inside and over forest: Influence on footprint prediction, *Bound.-Layer Meteorol.*, 109, 163–189, 2003.
- Rannik, Ü., Sogachev, A., Foken, T., Göckede, M., Kljun, N., Leclerc, M. Y., and Vesala, T.: Footprint Analysis, edited by: Aubinet, M., Vesala, T., Papale, D., in: *Eddy Covariance Handbook*, Springer, 211–261, 2012.
- Rinne, J., Hakola, H., Laurila, T., and Rannik, Ü.: Canopy scale monoterpene emissions of *Pinus sylvestris* dominated forests, *Atmos. Environ.*, 34, 1099–1107, 2000.
- Rinne, H. J. I., Guenther, A. B., Greenberg, J. P., and Harley, P. C.: Isoprene and monoterpene fluxes measured above Amazonian rainforest and their dependence on light and temperature, *Atmos. Environ.*, 36, 2421–2426, 2002.
- Rinne, J., Taipale, R., Markkanen, T., Ruuskanen, T. M., Hellén, H., Kajos, M. K., Vesala, T., and Kulmala, M.: Hydrocarbon fluxes above a Scots pine forest canopy: measurements and modeling, *Atmos. Chem. Phys.*, 7, 3361–3372, doi:10.5194/acp-7-3361-2007, 2007.
- Rinne, J., Bäck J., and Hakola, H.: Biogenic volatile organic compound emissions from Eurasian taiga: Current knowledge and future directions, *Boreal Environ. Res.*, 14, 807–826, 2009
- Ruuskanen, T. M., Müller, M., Schnitzhofer, R., Karl, T., Graus, M., Bamberger, I., Hörtnagl, L., Brilli, F., Wohlfahrt, G., and Hansel, A.: Eddy covariance VOC emission and deposition fluxes above grassland using PTR-TOF, *Atmos. Chem. Phys.*, 11, 611–625, doi:10.5194/acp-11-611-2011, 2011.
- Shu, Y. and Atkinson, R.: Atmospheric lifetimes and fates of a series of sesquiterpenes. *J. Geophys. Res.*, 100, 7275–7281, 1995.
- Strong, C., Fuentes, J. D., and Baldocchi, D.: Reactive hydrocarbon footprints during canopy senescence, *Agric. For. Meteorol.*, 127, 159–173, 2004.
- Stull, R. B.: *An Introduction to Boundary Layer Meteorology*. Kluwer Academic Publishers, Dordrecht, The Netherlands, 666 pp., 1988.
- Taipale, R., Kajos, M. K., Patokoski, J., Rantala, P., Ruuskanen, T. M., and Rinne, J.: Role of de novo biosynthesis in ecosystem scale monoterpene emissions from a boreal Scots pine forest, *Biogeosciences*, 8, 2247–2255, doi:10.5194/bg-8-2247-2011, 2011.
- Tanner, D., Jefferson, A., and Eisele, F.: Selected ion chemical ionization mass spectrometric measurement of OH. *J. Geophys. Res.*, 102, 6415–6425, 1997.
- Thomson, D. J.: Criteria for the selection of stochastic models of particle trajectories in turbulent flows. *J. Fluid. Mech.* 180, 529–556, 1987.
- Vesala, T., Kljun, N., Rannik, Ü., Rinne, J., Sogachev, A., Markkanen, T., Sabelfeld, K., Foken, Th., and Leclerc, M. Y.: Flux and concentration footprint modelling: State of the art. *Environ. Poll.*, 152, 653–666, 2008.
- Williams, J., Crowley, J., Fischer, H., Harder, H., Martinez, M., Petäjä, T., Rinne, J., Bäck, J., Boy, M., Dal Maso, M., Hakala, J., Kajos, M., Keronen, P., Rantala, P., Aalto, J., Aaltonen, H., Paatero, J., Vesala, T., Hakola, H., Levula, J., Pohja, T., Herrmann, F., Auld, J., Mesarchaki, E., Song, W., Yassaa, N., Nölscher, A., Johnson, A. M., Custer, T., Sinha, V., Thieser, J., Pouvesle, N., Taraborrelli, D., Tang, M. J., Bozem, H., Hosaynali-Beygi, Z., Axinte, R., Oswald, R., Novelli, A., Kubistin, D., Hens, K., Javed, U., Trawny, K., Breitenberger, C., Hidalgo, P. J., Ebben, C. J., Geiger, F. M., Corrigan, A. L., Russell, L. M., Ouwersloot, H. G., Vilà-Guerau de Arellano, J., Ganzeveld, L., Vogel, A., Beck, M., Bayerle, A., Kampf, C. J., Bertelmann, M., Köllner, F., Hoffmann, T., Valverde, J., González, D., Riekkola, M.-L., Kulmala, M., and Lelieveld, J.: The summertime Boreal forest field measurement intensive (HUMPPA-COPEC-2010): an overview of meteorological and chemical influences, *Atmos. Chem. Phys.*, 11, 10599–10618, doi:10.5194/acp-11-10599-2011, 2011.